J. Innovative Eng. Nat. Sci., vol. 6, no. 1, pp. 275-294, 2026.
http://doi.org/10.61112/jiens.1806895

Journal of Innovative Engineering and Natural Science
(Yenilikçi Mühendislik ve Doğa Bilimleri Dergisi)
https://dergipark.org.tr/en/pub/jiens

Original Paper

Seismic behavior of a RC column subjected to cyclic lateral loading after high temperature

Halit Erdem Çolakoğlu[a,*] Metin Hüsem[b]

[a]Giresun University, Keşap Vocational School Department of Construction, Giresun 28100, Türkiye.
[b]Karadeniz Technical University, Faculty of Engineering Department of Civil Engineering, Trabzon 61100, Türkiye.

ARTICLE INFO

Article history:
Received October 19, 2025
Received in revised form December 15, 2025
Accepted January 13, 2026

Available online

Keywords:
Structural behavior
High temperature
Reinforced concrete column
Finite element model (FEM)
Cyclic loading

ABSTRACT

Temperature causes many physical and chemical changes and has a negative impact on reinforced concrete (RC) structures. Long-term exposure to high temperatures reduces the strength and durability of RC elements and alters their seismic behavior. This study investigates the post-fire response of an RC column exposed to 600, 800, and 1000 °C following the ISO 834 standard fire curve. After natural cooling, the column behavior under cyclic lateral loading was analyzed. A finite element model was developed in ABAQUS to perform thermal analyses, followed by cyclic structural analyses. The effects of high temperature were evaluated in terms of changes in lateral load-carrying capacity and stiffness under different axial load levels. The results show that increasing temperature leads to a continuous reduction in both lateral load-carrying capacity and stiffness. At 1000 °C, these reductions reach approximately 53% and 85%, respectively. Based on these findings, RC columns exposed to temperatures of 600 °C and above 180 minutes should not be reused without strengthening. This study provides practical support for the post-fire evaluation of reinforced concrete structural elements.

I. INTRODUCTION

Temperature, which is shown as the main cause of many physical and chemical events on earth, also negatively affects engineering structures. Changes in the mechanical properties of concrete and steel materials exposed to temperature effect cause strength and stiffness losses in reinforced concrete and elements.

In order to make sense of the effect of temperature on reinforced concrete (RC) structures and elements, it is necessary to investigate the effect of temperature on concrete and steel materials that make up RC structural elements. The resistance of concrete to high temperatures depends on factors such as aggregate and cement type and moisture content [1, 2]. As a general case, aggregates have high fire resistance, but cooling the concrete by spraying water or exposing it to thermal shocks by irregular heating increases the internal pressure in the aggregates and causes them to disintegrate. In addition, the grain size of the aggregate used in concrete production is also effective on high temperature performance [3, 4]. On the other hand, calcium hydroxide in the composition of the cement in concrete turns into calcium oxide when the temperature rises to 400 - 450 °C. Actions taken to cool the concrete accelerate the formation of calcium hydroxide again. The volume changes that occur because of this transformation can also cause concrete to disintegrate [5-8]. If the temperature exceeds 300 °C, the yield and tensile strength of reinforced concrete steel decreases. Between 600 - 1200 °C, it is known that plastic deformations occur in the steel material [9]. According to these studies in literature, it can be said that the damage to RC structures and elements exposed to high temperatures varies depending on the degree and duration of the

*Corresponding author. Tel.: +90-530-959-2315; e-mail: erdem.colakoglu@giresun.edu.tr

temperature. In these studies, it is known that the degree of temperature and duration of action affect the extent of damage by changing the physical, chemical and mineralogical properties of concrete [10, 11].

Another factor that is effective in the extent of damage to RC structures and elements exposed to high temperatures is the heating rate. In fact, the change in the heating rate in RC structures and elements will cause thermal shock effect, which significantly increases high temperature damage. Gautam et al [12] heated two types of granite rocks to 300 °C at four different heating rates (3, 5, 10 and 15 °C/min). In the study, it was determined that thermal cracks started to form when the heating rate exceeded 3 - 5 °C/min on average. It was found that the heating rate should not exceed 5 °C/min to prevent thermal shock damage. Li et al [13] studied the effect of heating rate on the free expansion deformation of concrete. In the 100 - 800 °C range, it was determined that the deformations due to expansion increased gradually with the increase in the heating rate. It was determined that the deformation of the concrete, especially in the range of 100 - 400 °C, was slightly affected by the heating rate. In the range of 500 - 800 °C, it was found that there is a linear relationship between heating rate and deformation due to expansion [13].

As can be seen from the studies in the literature, it is determined that the negative effect of high temperature on RC structures and elements varies depending on the physical, chemical and mineralogical properties of concrete and steel materials, as well as the degree and duration of the temperature. In these studies, rather than the behavior of RC structures and elements, the change in the mechanical properties of concrete and steel materials after high temperature effect has been discussed. It has been determined that the effect of high temperature significantly affects the modulus of elasticity and strength of concrete and causes strength depletion in concrete and steel by reducing the yield and ultimate strength and bond strength of steel reinforcement [14-18]. However, these studies are mostly focused on the change in material properties and do not include the seismic performance of RC structures or elements exposed to high temperatures.

Some of the studies in the literature have investigated the mechanical performance of structural elements such as RC beams, columns and slabs exposed to high temperatures. Chen et al. [19] investigated the effect of fire exposure time on the structural behavior of RC columns after fire. Nine full-scale RC columns were tested under axial load and bending after exposure to high temperature for 2 and 4 hours in accordance with ISO 834 standard fire curve. Test results show that the residual load carrying capacity decreases with increasing fire exposure time. In studies in literature, it has also been determined that load carrying capacity decreases with the increase in the duration of exposure to high temperature [20-24]. However, in these studies, only the duration of high temperature effect was considered as a variable parameter. Therefore, since all samples were subjected to equal ambient temperature, the studies were limited in this aspect.

When the related studies in literature are examined, it is seen that the axial load level and eccentricity are also effective in the change in the structural behavior of RC columns exposed to high temperatures. Pul et al. [25] aimed to characterize the structural behavior of a RC column subjected to 1150 °C high temperature and axial load simultaneously subjected to different heating and cooling scenarios. In this direction, a constant axial load was applied during the heating process lasting 30, 60 and 120 minutes and the change in the bearing capacity and stiffness of the RC column was investigated. As a result of the study, it was determined that the axial load carrying capacity can decrease up to 35% if the high temperature is effective for 120 minutes. However, the change in the lateral load carrying capacity of a RC column exposed to high temperature was not addressed in the study.

Therefore, no evaluation was made for the columns that will be exposed to earthquake effect after high temperature.

The originality of this study lies in its numerical investigation of the post-fire seismic behavior of reinforced concrete columns by simultaneously considering fire temperature level, exposure duration, and axial load ratio. Most existing studies in literature primarily focus on the effects of high temperature on material properties or residual load-carrying capacity, while the behavior of reinforced concrete columns under cyclic lateral loading after fire exposure has received limited attention. Moreover, studies that systematically evaluate the combined influence of different temperature levels and axial load ratios on lateral load-carrying capacity and stiffness degradation are scarce. In this respect, the present study provides a comprehensive thermo-mechanical assessment based on the ISO 834 [26] standard fire curve and addresses a clear gap in the existing literature.

The aim of this study is to evaluate the behavior of a reinforced concrete column exposed to temperatures of 600, 800, and 1000 °C for a specified duration and subsequently subjected to earthquake-representative cyclic lateral loading after natural cooling. The changes in lateral load-carrying capacity and stiffness are numerically examined for different axial load levels. The findings are intended to directly support performance-based post-fire assessment, strengthening, and reuse decisions for reinforced concrete columns, thereby offering practical value for both researchers and practicing structural engineers.

II. EXPERIMENTAL METHOD / TEORETICAL METHOD

In this study, the behavior of a RC column subjected to 600, 800 and 1000 °C high temperatures under a constant axial load and cyclic lateral load were investigated using ABAQUS [27] package program. The study was carried out in three stages, and the flow chart is shown in Figure 1. In the first stage, the finite element model of the RC column was created by determining the size, cross-sectional properties and reinforcement details. In the second stage, the finite element model of the RC column was subjected to different degrees of high temperature (600, 800, 1000 °C) and thermal analysis was performed. In the third stage, structural analyses of the RC column element, which cooled after thermal analysis, were carried out with constant axial load levels of 85%, 20% and 0% of the axial load capacity of the RC column element under the effect of cyclic lateral load.

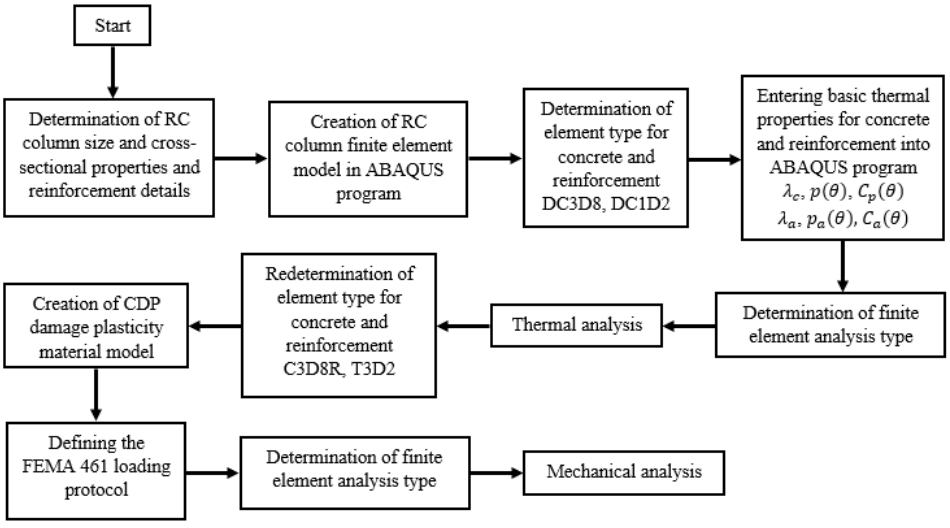

Figure 1. Flowchart showing the design, thermal and mechanical analysis stages of RC column

2.1 Determination of dimensional and cross-sectional properties and reinforcement details of RC column and creation of finite element model

The dimensions, cross-sectional properties and reinforcement details of the RC column used in the study were determined in 1/1 scale in accordance with TBDY-2018 [28] and shown in Figure 2.

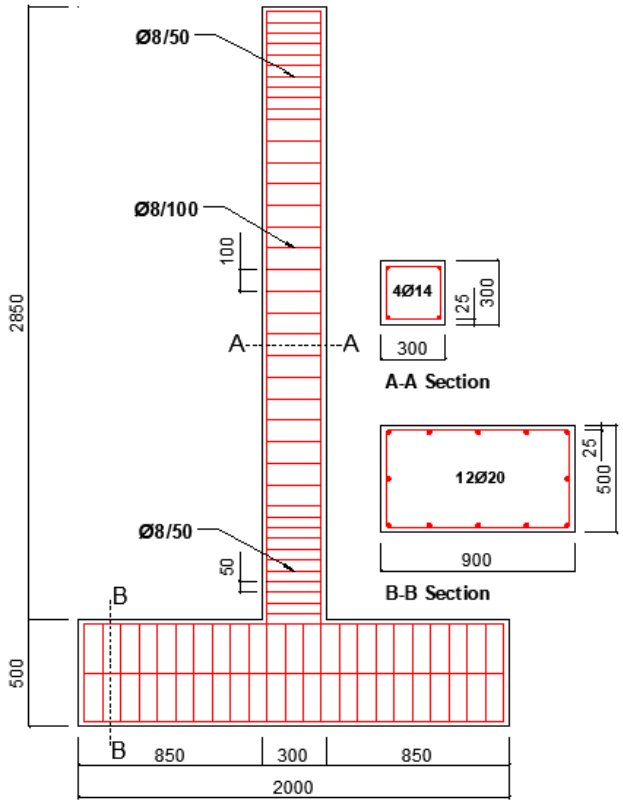

Figure 2. RC column size, cross-section and reinforcement details (All dimensions are in mm)

Four 14mm diameter longitudinal reinforcements and 8 mm diameter transverse reinforcements were used in the RC column. A 500 mm long wrapping zone was formed at the bottom and end of the column and transverse reinforcements were placed at 50 mm distances in this zone. Transverse reinforcement at 100 mm distances was used in the body part of the RC column. The RC column is supported on a single foundation with dimensions of 900x500x2000 mm (width, height, length). In the foundation, 12 longitudinal reinforcements with a diameter of 20 mm were used and transverse reinforcements with a diameter of 8mm were placed at 85 mm distances.

RC columns and foundations are made of concrete with C25/30 strength class (C25/30; 28-day characteristic cylinder and cube compressive strength of 25 and 30 MPa respectively). Mechanical properties of concrete and reinforcement materials are shown in Table 1.

Table 1. Mechanical properties of concrete and reinforcement materials

CONCRETE				
Density (kg/m^3)		2550		
Compressive strength (MPa)		25		
Poisson ratio		0.2		
STEEL REBARS	**Ø8**	**Ø10**	**Ø14**	**Ø20**
Density (kg/m^3)	7850	7850	7850	7850
Poisson ratio	0.3	0.3	0.3	0.3
Elastic modulus (GPa)	200	200	200	200
Yield stress (MPa)	420	420	420	420

The finite element model of the RC column, whose dimensional and cross-sectional properties and reinforcement details were determined, was created using ABAQUS [27] program. In numerical analysis using the finite element method, the dimensions of the element considered are extremely important in determining the analysis time. Reducing the finite element size leads to a longer analysis time and increasing the finite element size leads to a shorter analysis time. In this direction, in the present study, while creating the finite element model of the RC column, it was tried to determine the finite element mesh that would not extend the analysis time too much and the crushing and cracking in the concrete could be observed in the best way. For this purpose, the finite element mesh of the RC column was created using hexahedral mesh with dimensions of 100x100 mm (Figure 3). Since the thermal analysis of the RC column exposed to high temperatures of 600, 800 and 1000 °C in the first stage will be carried out in the study, the 8-node continuous heat transfer element (DC3D8) type was selected to best reflect the results of the effects of high temperature on the concrete material. In the numerical modeling of the transverse and longitudinal reinforcement of the RC column, a heat transfer element (DC1D2) type with 2 nodes was used. After thermal analysis, structural analysis of the RC column under cyclic lateral load was carried out. In these analyses, the 3-dimensional and 8-node continuous solid element (C3D8R) type was preferred, which best simulates the load effects, displacements, plastic deformations, cracking and crushing behavior of concrete (Figure 4a). In order to simulate the transverse and longitudinal reinforcement in the structural analysis, a 2-node, 3-dimensional bar element (T3D2) type was used (Figure 4b).

In the study, an RC column was anchored to the ground from the foundation part and a reference point was established for the application of lateral load. Lateral load was applied through this point. In order to prevent out-of-plane behavior of the column under the cyclic lateral load, the displacements in the z direction were closed (Figure 4).

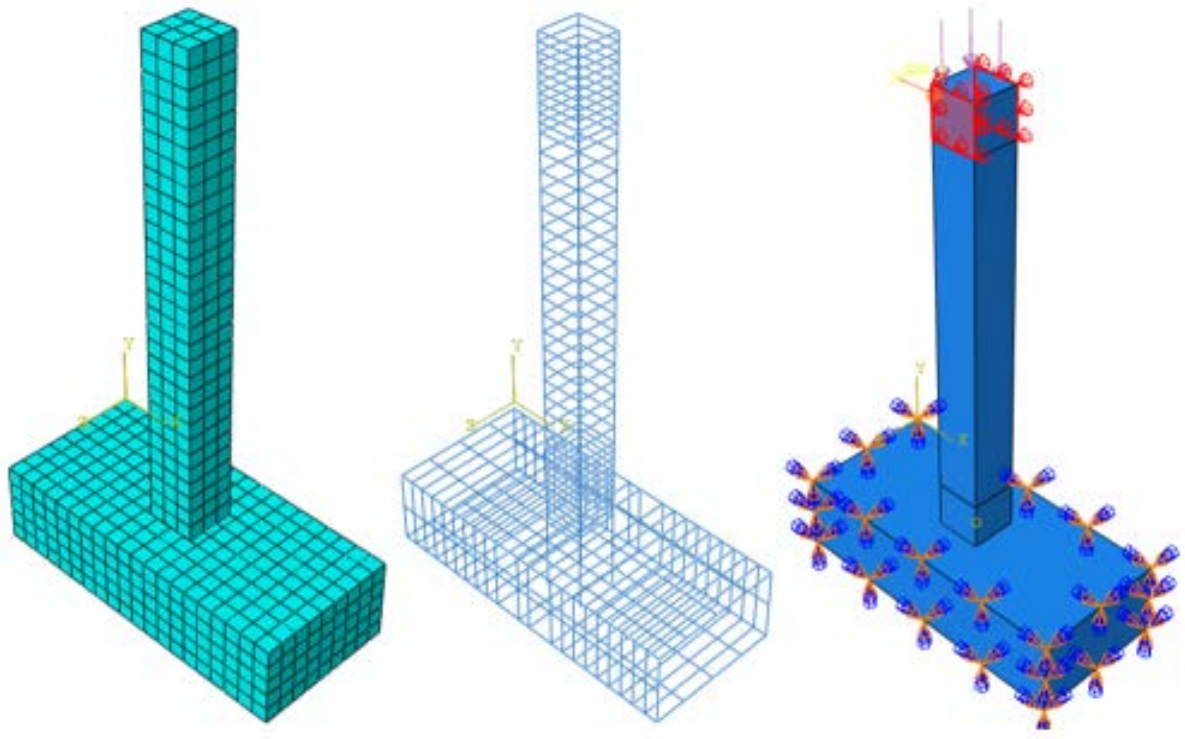

Figure 3. Application of lateral and axial load with finite element model of RC column

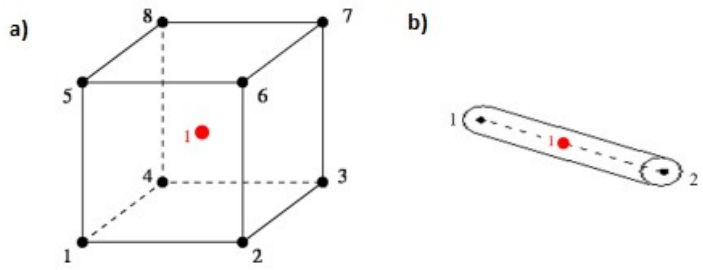

Figure 4. a) C3D8R element b) T3D2 element [27]

2.2 Thermal analysis of RC column

In the ABAQUS [27] package program, three basic thermal properties of concrete and steel materials must be defined in the program in thermal analysis where high temperature effect is applied to the RC column. These thermal properties of concrete and steel are coefficient in thermal conductivity, density and specific heat.

The thermal conductivity coefficient of concrete (λ_c) was calculated using Eq. 1 and Eq. 2 for the upper limit and lower limit, respectively, as specified in TS EN 1992-1-2 [29] (Figure 5).

$$\lambda_c = 2 - 0.2451(\theta/100) + 0.0107(\theta/100)^2 \qquad 20℃ \leq \theta \leq 1200℃ \tag{1}$$

$$\lambda_c = 1.36 - 0.136(\theta/100) + 0.0057(\theta/100)^2 \qquad 20℃ \leq \theta \leq 1200℃ \tag{2}$$

The change in concrete density with temperature was calculated using Eq. 3-6, as specified in TS EN 1992-1-2 [29] (Figure 4). Here p is the density of concrete.

$$p(\theta) = p(20℃) \qquad 20\ ℃ \leq \theta \leq 115\ ℃ \tag{3}$$

$$p(\theta) = p(20℃)(1 - 0.02(\theta - 115)/85) \qquad 115\ ℃ < \theta \leq 200\ ℃ \tag{4}$$

$$p(\theta) = p(20℃)(0.98 - 0.03(\theta - 200)/200) \qquad 200\ ℃ < \theta \leq 400\ ℃ \tag{5}$$

$$p(\theta) = p(20℃)(0.95 - 0.07(\theta - 400)/800) \qquad 400\ ℃ < \theta \leq 1200\ ℃ \tag{6}$$

The change of concrete specific heat with temperature was calculated using Eq. 7-10, as specified in TS EN 1992-1-2 [29] (Figure 5). Here C_p is the specific heat of concrete.

$$C_p(\theta) = 900 \qquad 20\ ℃ \leq \theta \leq 115\ ℃ \tag{7}$$

$$C_p(\theta) = 900 + (\theta - 100) \qquad 100\ ℃ < \theta \leq 200\ ℃ \tag{8}$$

$$C_p(\theta) = 1000 + (\theta - 200)/2 \qquad 200\ ℃ < \theta \leq 400\ ℃ \tag{9}$$

$$C_p(\theta) = 1100 \qquad 400\ ℃ < \theta \leq 1200\ ℃ \tag{10}$$

The thermal conductivity coefficient of steel (λ_a) was calculated using Eq. 11 and Eq. 12 as specified in TS EN 1993-1-2 [30] (Figure 5). Here θ_a refers to the degree of temperature to which the steel is exposed.

$$\lambda_a = 54 - 3.33x10^{-2}\theta_a \qquad 20℃ \leq \theta_a < 800℃ \tag{11}$$

$$\lambda_a = 27.3 \qquad 800℃ \leq \theta_a \leq 1200℃ \tag{12}$$

Steel density is independent of temperature and can generally be taken as $p_a = 7850$ kg/m^3 (Figure 5). The change in the specific heat of steel with temperature was calculated using Eq. 13-16, as specified in TS EN 1993-1-2 [30] (Figure 5).

$$C_a = 425 + 7.73\ x\ 10^{-1}\theta_a - 1.69\ x\ 10^{-3}{\theta_a}^2 + 2.22\ x\ 10^{-6}{\theta_a}^3 \quad 20\ ℃ \leq \theta_a < 600\ ℃ \tag{13}$$

$$C_a = 666 + 13002/(738 - \theta_a) \qquad 600\ ℃ \leq \theta_a < 735\ ℃ \tag{14}$$

$$C_a = 545 + 17820/(\theta_a - 731) \qquad 735\ ℃ \leq \theta_a < 900\ ℃ \tag{15}$$

$$C_a = 650 \qquad 900\ ℃ \leq \theta_a \leq 1200\ ℃ \tag{16}$$

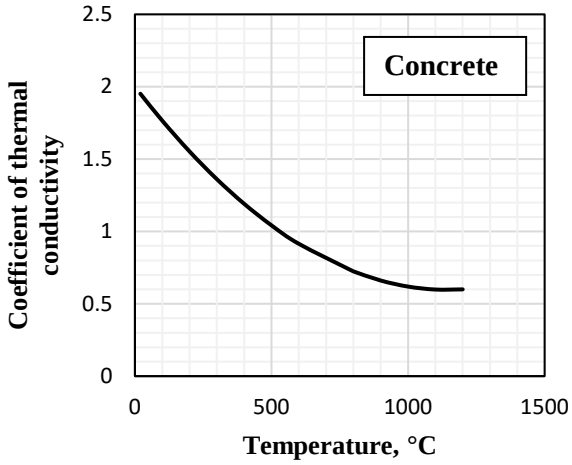

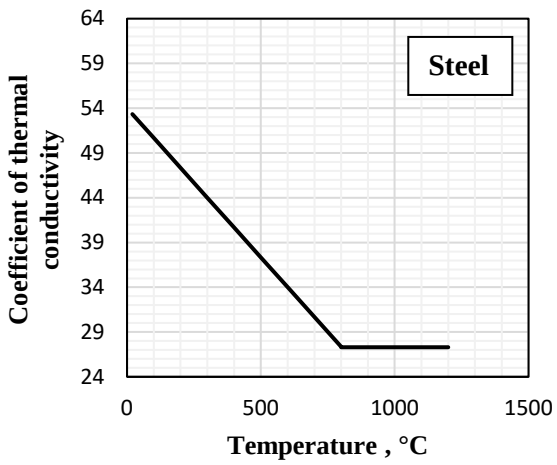

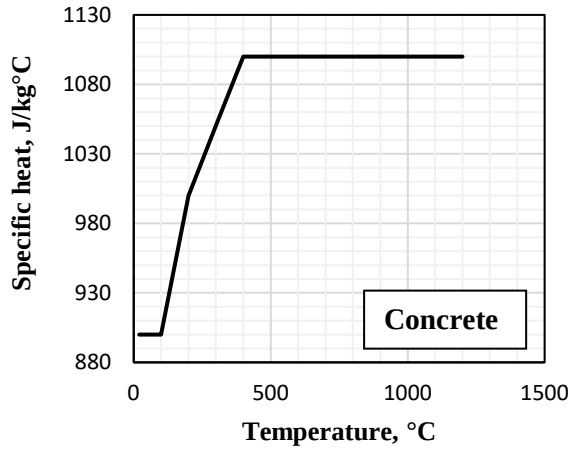

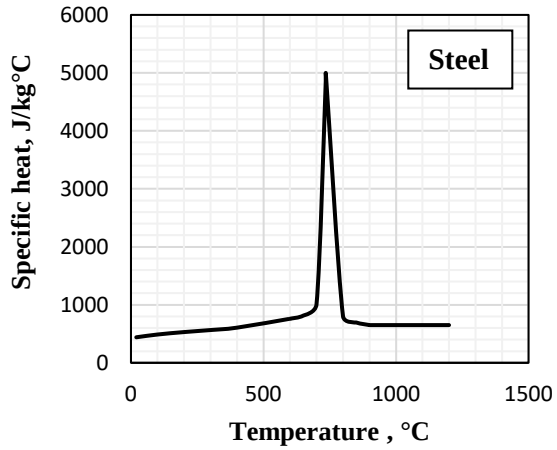

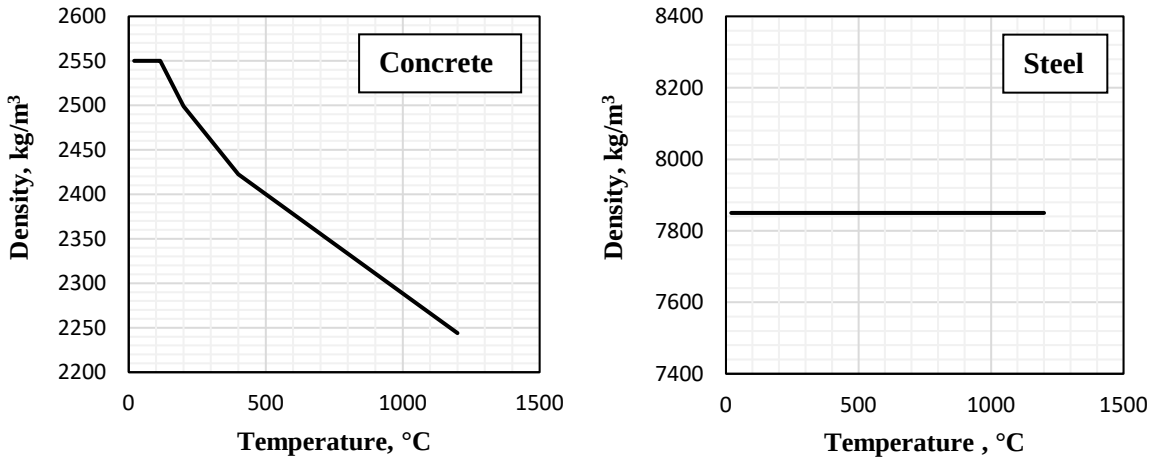

Figure 5. Basic thermal properties for concrete and steel

In the study, the RC column was exposed to temperatures of 600, 800 and 1000°C. The target temperatures determined in all column specimens were reached in accordance with the ISO 834 [26] standard fire curve (Figure 6). Once the target temperatures were reached, all samples were exposed to these target temperatures for 180 minutes (Table 2).

Table 2. Thermal analysis of RC column

Group no	*Temperature level (°C)*	*Heating time after the target temperature (min)*
1	600	
2	800	180
3	1000	
4	20	-

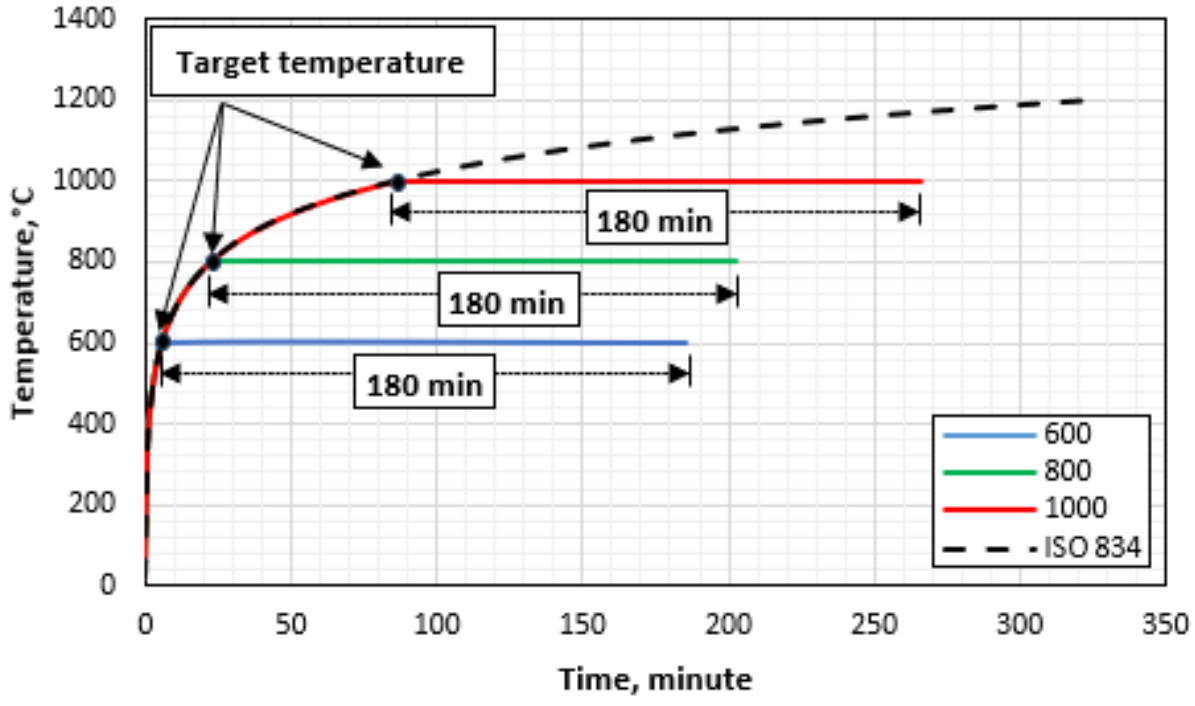

Figure 6. Application of high temperature effect in thermal analysis

2.3 Structural analysis of RC column

In order to fully simulate the actual properties of concrete and RC steel used as building materials in numerical studies, various material models should be used.

Since the RC column will be subjected to both pushing and pulling effects under cyclic lateral loading, modeling the cracking and crushing behavior of the concrete is of utmost importance. For this purpose, the cracking behavior of concrete due to crushing and tensile effects was simulated using the Concrete Damage Plasticity (CDP) material model in the ABAQUS [27] package program. Here CDP refers to the concrete damage plasticity material model used in ABAQUS software [27].

While creating the CDP material model, pressure effects were calculated in accordance with TS EN 1992-1-2 [29] as specified in Eq. 17. Here σ_θ is the stress in the mathematical model that determines the stress-strain relationship of concrete exposed to high temperature [29].

$$\sigma_\theta = \frac{3\varepsilon f_{c\theta}}{\varepsilon_{c1\theta}\left(2+\left(\frac{\varepsilon}{\varepsilon_{c1\theta}}\right)^3\right)} \tag{17}$$

Here $\varepsilon_{c1\theta}$ refers to the thermal unit deformation of concrete due to different temperatures, ε refers to the deformation of concrete and $f_{c\theta}$ refers to the compressive strength of concrete at different temperatures, and these values are given in Table 3 [29].

Table 3. Determination of the stress – strain relationship of concrete under high temperature

Determination of compressive strength				***Determination of tensile strength***			
$f_{c\theta}/f_{ck}$	$\varepsilon_{c1\theta}$	$\varepsilon_{cu1\theta}$	θ °C	$f_{ckt\theta}$	$k_{ct(\theta)}$	θ °C	f_{ckt}
1.00	0.0025	0.020	20	1.95	1	20	1.95
1.00	0.004	0.0225	100	1.95	1	100	1.95
0.97	0.0055	0.0250	200	1.9461	0.998	101	1.95
0.91	0.0070	0.0275	300	1.56	0.8	200	1.95
0.85	0.0100	0.0300	400	1.17	0.6	300	1.95
0.74	0.0150	0.0325	500	0.78	0.4	400	1.95
0.60	0.0250	0.0350	600	0.39	0.2	500	1.95
0.43	0.0250	0.0375	700	0	0	600	1.95
0.27	0.0250	0.0400	800				
0.15	0.0250	0.0425	900				
0.06	0.025	0.045	1000				

Tensile effects in the CDP material model applied by reducing the characteristic tensile strength (f_{ckt}) of concrete using Eq. 18 in accordance with TS EN 1992-1-2 [29]. Here $k_{ct}(\theta)$, is the change of the reduction coefficient with temperature and was determined using Eq. 19-20.

$$f_{ckt}(\theta) = k_{ct}(\theta) f_{ckt} \tag{18}$$

$$k_{ct}(\theta) = 1.0 \qquad 20°C \le \theta \le 100°C \tag{19}$$

$$k_{ct}(\theta) = 1.0 - 1.0\,(\theta - 100)/500 \qquad 100°C < \theta \le 600°C \tag{20}$$

The pressure and tensile effects defined in the CDP material model shown in Figure 7a and Figure 7b, respectively.

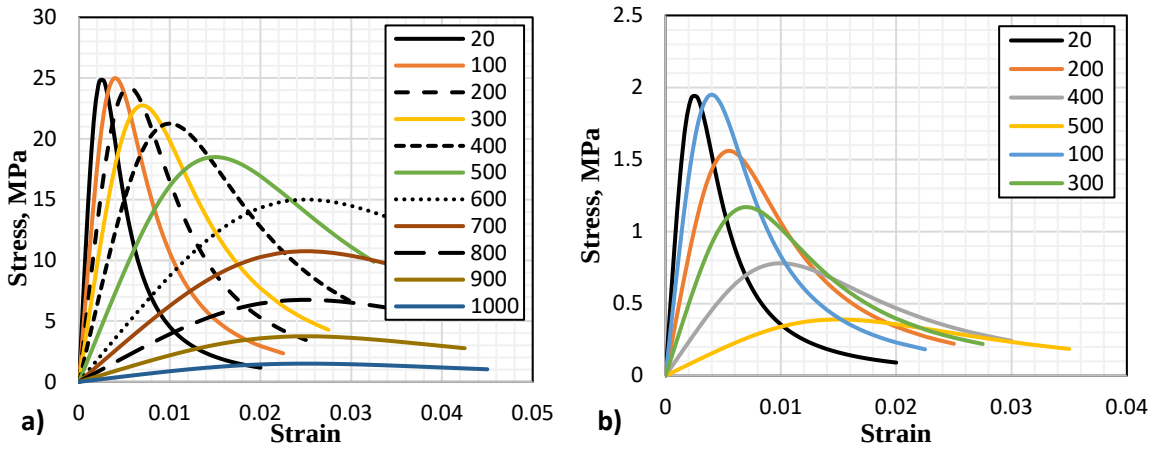

Figure 7. Idealized stress – strain curves of concrete a) For axial compression b) For axial tension

Cracks occurring in the RC column under cyclic lateral load cause a decrease in the stiffness of the column. In the ABAQUS [27] package program, these reductions in stiffness are simulated using stiffness reduction parameters dc for compression and dt for tension. The stiffness losses in the RC column as a result of inelastic deformations are shown in Figure 8.

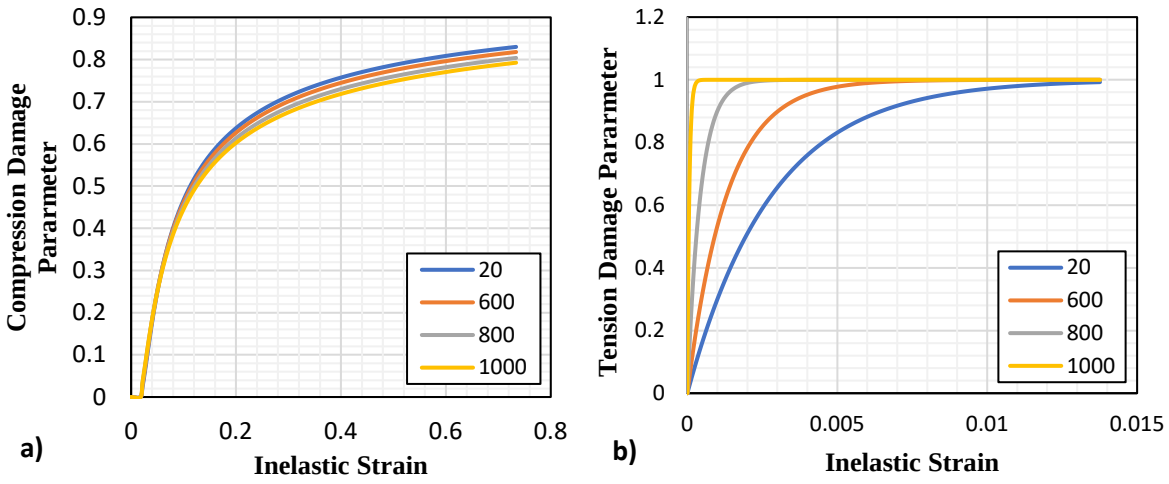

Figure 8. Change of stiffness reduction parameter due to inelastic deformation a) for compression b) for tension

For the CDP material model used in line with finite element modelling, the parameters defined as dilation angle (ψ), eccentricity (e), viscosity (μ), the ratio of the yield stress in biaxial loading to the yield stress in uniaxial loading case f_{bo}/f_{co} must be entered into the ABAQUS package program [27].

Dilation angle (ψ), is the numerical expression of the volumetric change in the material under shear stress or shear deformation. Changing the dilation angle may result in more rigid or more elastic material behaviour under the same deformations. In many studies in the literature [31–35], the dilation angle was chosen between 5° and 45°, aiming to be compatible with experimental studies. Based on parametric studies in the literature [35], it was decided to take the dilatation angle as 32° in the present study (Figure 9). Increasing the dilation angle causes the material to exhibit more rigid behavior and gradually increases the lateral load carrying capacity (Figure 9).

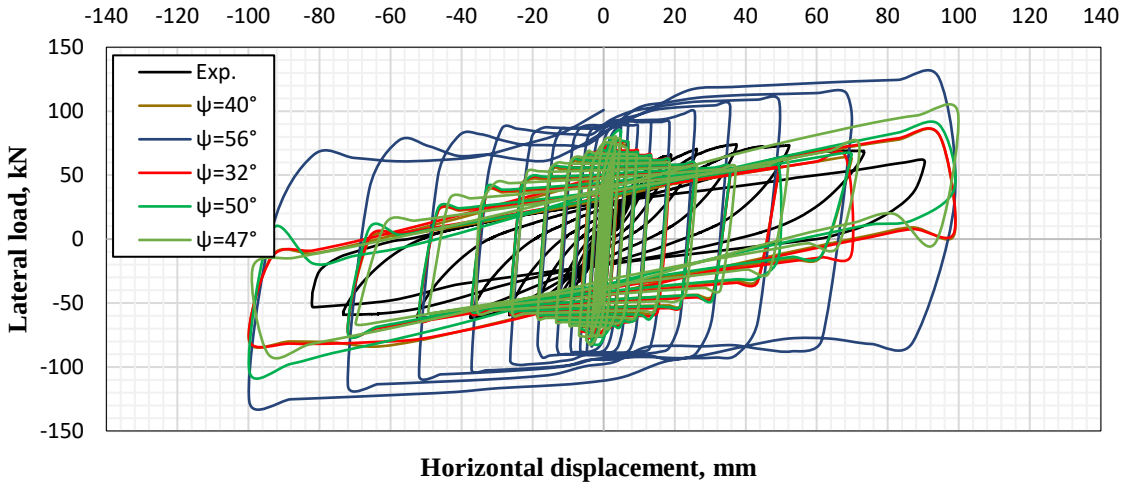

Figure 9. Effect of change of dilation angle on lateral load - horizontal displacement relationship [34]

Eccentricity (e), is a small positive number that describes the speed at which the hyperbolic flow potential approaches its asymptote [27]. As the eccentricity approaches zero, the flow potential becomes a straight line. The default eccentricity used in the literature [36, 37] and in this study was taken as 0.1.

The ratio f_{bo}/f_{co} defined as the ratio of the yield stress in biaxial loading to the yield stress in uniaxial loading, taken as 1.16 in the literature [38, 39] and in this study.

Viscosity (μ), is the parameter that enables the concrete material equations to be arranged as visco-plastic in numerical analyses. Softening and stiffness losses occurring in cross-sections in material models create convergence problems in analyses, and the viscosity parameter ensures that such problems are minimized. The default viscosity value by the ABAQUS package program is 0, and in studies in the literature [27, 36, 37, 40, 41] the viscosity value was chosen between 1×10^{-7} and 667×10^{-3}. Based on parametric studies in the literature [35], it was decided to take the viscosity as 1×10^{-4} in the present study (Figure 10). Increasing the viscosity value from 10^{-4} to 10^{-3} minimizes the softening and stiffness losses occurring in the material, thus greatly increasing the lateral load carrying capacity [35].

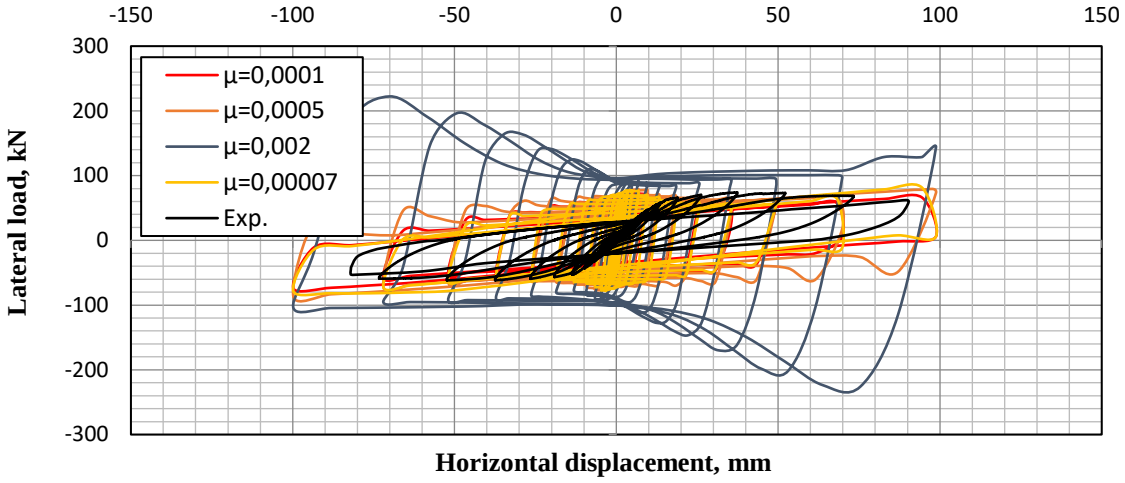

Figure 10. Effect of viscosity change on lateral load - horizontal displacement relationship [35]

In many studies in the literature [40-43], RC steel has been modeled using the elastoplastic material model. In the present study, the mechanical properties of the steel members shown in Table 1 were simulated with the elastoplastic material model. According to this model, after the steel reaches its yield strength, it undergoes plastic deformation without any stress increase (Figure 11). The elastoplastic material model is defined by entering the yield strength, Poisson's ratio, modulus of elasticity and plastic deformation parameters of steel into the ABAQUS program.

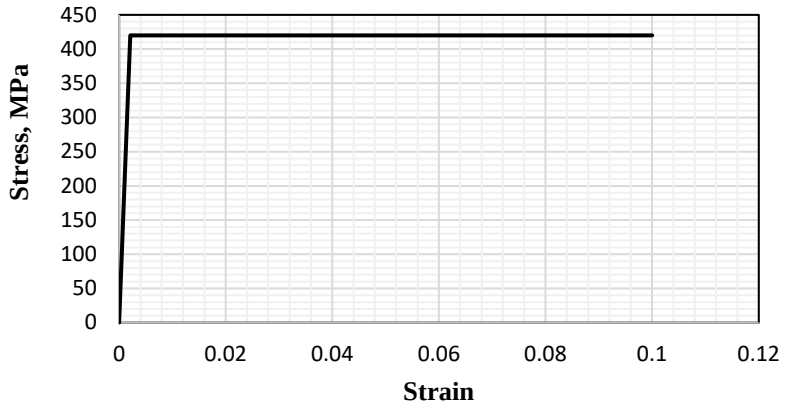

Figure 11. Stress – strain relationship of steel reinforcement

Since the RC column subjected to 600, 800 and 1000°C temperature effects was then examined under cyclic lateral load, the mechanical analysis method was chosen. A quasi-static loading protocol was applied to the finite element modeled RC columns in accordance with FEMA 461 [44]. A cyclic loading protocol was prepared by increasing the horizontal displacement applied for the first 6 cycles by 40% for each subsequent cycle as specified in FEMA 461 [44] (Figure 12).

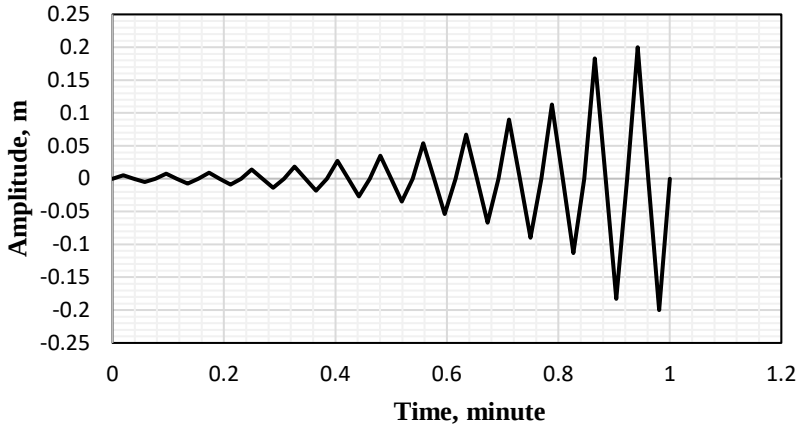

Figure 12. Quasi-static loading protocol prepared according to FEMA 461

After the thermal analysis of the RC column, a nomenclature such as Exposed Temperature - Percentage of Axial Load Capacity and N (Axial load) was used to avoid confusion in the mechanical analysis applied. Accordingly, Table 4 shows the analysis matrix used in the study.

Table 4. Analysis matrix used in the study

Group No	*Temperature level (°C)*	*Heating time after the target temperature (min)*	*Axial Load (kN)*	*Sample name*
1	600	180	1147.5	600-%85N
			270	600-%20N
			0	600-%0N
2	800	180	1147.5	800-%85N
			270	800-%20N
			0	800-%0N
3	1000	180	1147.5	1000-%85N
			270	1000-%20N
			0	1000-%0N
4	20	-	1147.5	Ref-%85N
			270	Ref-%20N
			0	Ref-%0N

III. RESULTS AND DISCUSSIONS

3.1 Thermal analysis of RC column

The RC column, whose finite element model was made using ABAQUS program, was heated for 180 minutes at these target temperatures after reaching the targeted 600, 800 and 1000 °C temperature effect in accordance with the ISO 834 [26] standard fire curve. As a result of the thermal analysis, the distribution of the target temperatures in the RC column body section was obtained (Figure 13).

In the thermal analysis, the RC column was exposed to high temperatures affecting all surfaces. According to the analytical temperature profiles obtained from thermal analysis, it is clearly seen that the target temperature moves towards the center of the column cross-section as the degree of applied temperature increases (Figure 13). It can be said that the change in temperature distribution within the concrete cross-section depends on a certain thermal conductivity property of concrete.

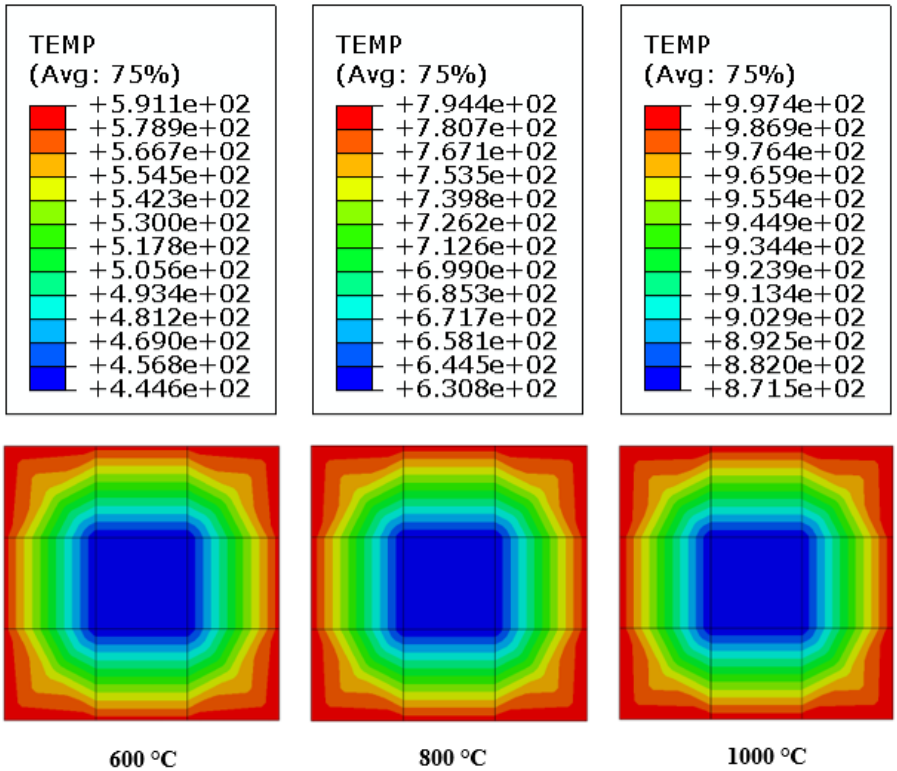

Figure 13. Temperature distribution in RC column body section

In the current study, the RC column was subjected to mechanical analysis where it was subjected to cyclic lateral load effect after thermal analysis where it was exposed to high temperature. In these sequential analyses expressed as thermo-mechanical analysis, it is extremely important for the reliability of the study that the RC column to which mechanical analysis is applied fully includes the effect of thermal damage. In the present study, the RC column was exposed to ambient temperatures of 600, 800 and 1000 °C and the distribution of temperature within the column cross-section is as shown in Figure 13. After reaching the target temperatures determined in the thermal analysis in accordance with the ISO 834 [26] standard fire curve, these target temperatures were kept constant for 180 minutes. The ABAQUS software completes this heating process in a specific incremental step. Mechanical analysis is performed by processing the ABAQUS file of the thermal analysis to the file of the mechanical analysis as initial data with the number of incremental steps in which the thermal analysis is completed. Thus, fire damage to the RC column as a result of thermal analysis is considered in the cyclic lateral load analysis.

3.2 Lateral load - horizontal displacement curve of RC column

After thermal analysis, the RC column was also subjected to cyclic lateral loading in accordance with the quasi-static loading protocol shown in Figure 12. Three different axial load levels (85%N, 20%N, 0%N) were considered to investigate the effect of temperature on the lateral load carrying capacity of the RC column during the application of the lateral load effect. Axial load levels were defined by the axial load ratio, i.e. the ratio of the applied axial load to the gross concrete axial load capacity. In this study, 20%N axial load level is used as the limit value for columns made of normal strength concrete. 85%N axial load level is considered as a possible value during severe earthquakes [45]. In addition to this, the axial load level of 0N% is considered as the case where there is no axial load. In this direction, the variation of the lateral load - horizontal displacement relations obtained as a result of the thermo - mechanical analysis of the RC column with temperature for different axial load levels is shown in Figure l4.

According to Figure 14, the lateral load carrying capacity of the RC column not subjected to high temperature increases with the increase in axial load level. Since axial load prevents the opening and deepening of cracks in the RC column bearing area under the effect of cyclic lateral load, it improves the lateral load carrying capacity. In this direction, the horizontal load carrying capacity of the Ref-%85N element, where 85% of the column axial load capacity was applied, was determined as 16278 N in push and 16791 N in pull. In the case of Ref-%0N without axial load, the horizontal load carrying capacity of the RC column decreases by 29.47% compared to Ref-%85N. Many studies in literature also support this finding from the present study [46].

On the other hand, numerical data on the lateral load carrying capacity of the column subjected to high temperature effect for the cases where an axial load of 85%, 20% and 0% of the column axial load capacity is applied together with the cyclic lateral load are shown in Table 5.

According to Table 5, the lateral load carrying capacity of the 600-%85N column elements after high temperature decreased by 17.69% in thrust and 17.83% in tension compared to the Ref-%85N reference element not exposed to high temperature. This decrease was determined to be 29.21% in pushing and 29.72% in pulling for the 800-%85N column element and 53.91% in pushing and 70.83% in pulling for the 1000-%85N column element (Figure 15).

The lateral load carrying capacity of the 600-%20N column elements after high temperature decreased by 25.67% in pushing and 25.35% in pulling compared to the Ref-%20N reference element not exposed to high temperature. This decrease was determined to be 42.42% in push and 42.30% in pull for the 800-20N column element and 48.27% in push and 48.25% in pull for the 1000-%20N column element (Figure 15).

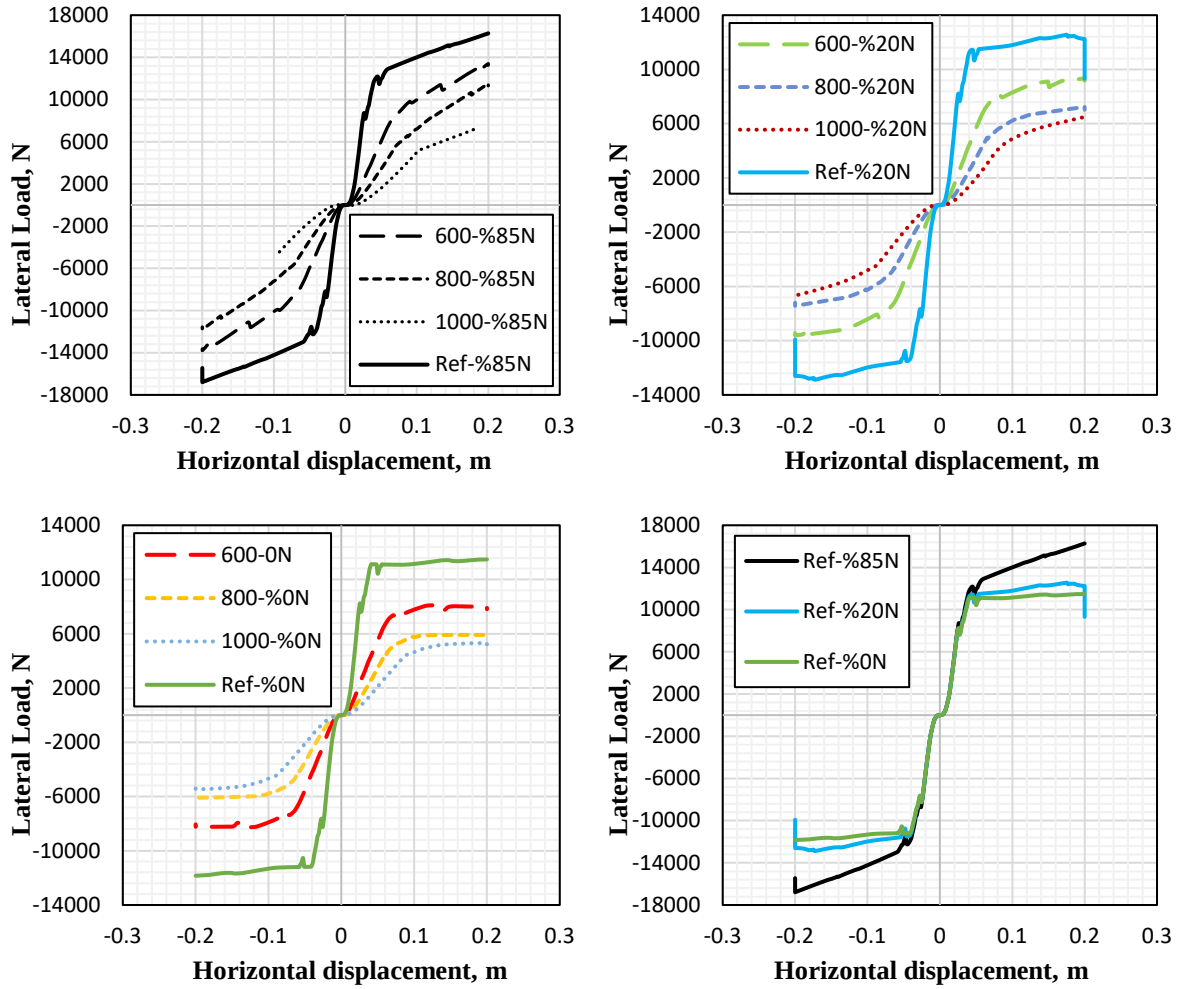

Figure 14. Temperature dependent variation of lateral load carrying capacity of RC column

Table 5. Variation of lateral load carrying capacity with temperature and axial load

Group No	*Sample Name*	*Push*	*Pull*	*Section Effect (N)*	*Temperature Effect (N)*	*Axial Load Effect (N)*
1	600-%85N	13397.36	-13797.72	11481.27	-2880.31	4796.39
	800-%85N	11523.74	-11801.61	11481.27	-4753.92	4796.39
	1000-%85N	7502.78	-4897.95	11481.27	-8774.89	4796.39
2	600-%20N	9334.77	-9617.00	11481.27	-3223.90	1077.40
	800-%20N	7231.25	-7432.77	11481.27	-5327.42	1077.40
	1000-%20N	6496.68	-6666.43	11481.27	-6061.99	1077.40
3	600-%0N	8097.13	-8268.78	11481.27	-3384.14	0.00
	800-%0N	5916.89	-6095.34	11481.27	-5564.38	0.00
	1000-%0N	5303.39	-5457.84	11481.27	-6177.88	0.00
4	Ref-%85N	16277.66	-5457.84	11481.27	-6177.88	0.00
	Ref-%20N	12558.67	-16791.24	11481.27	0.00	4796.39
	Ref-%0N	11481.27	-12882.27	11481.27	0.00	1077.40

The lateral load carrying capacity of the 600-%0N column elements without axial load after high temperature decreased by 29.48% in pushing and 30.17% in pulling compared to the Ref-%0N reference element which was

not exposed to high temperature. This decrease was determined as 48.46% in push and 48.52% in pull for the 800-%0N column element and 53.81% in push and 53.91% in pull for the 1000-%0N column element (Figure 15).

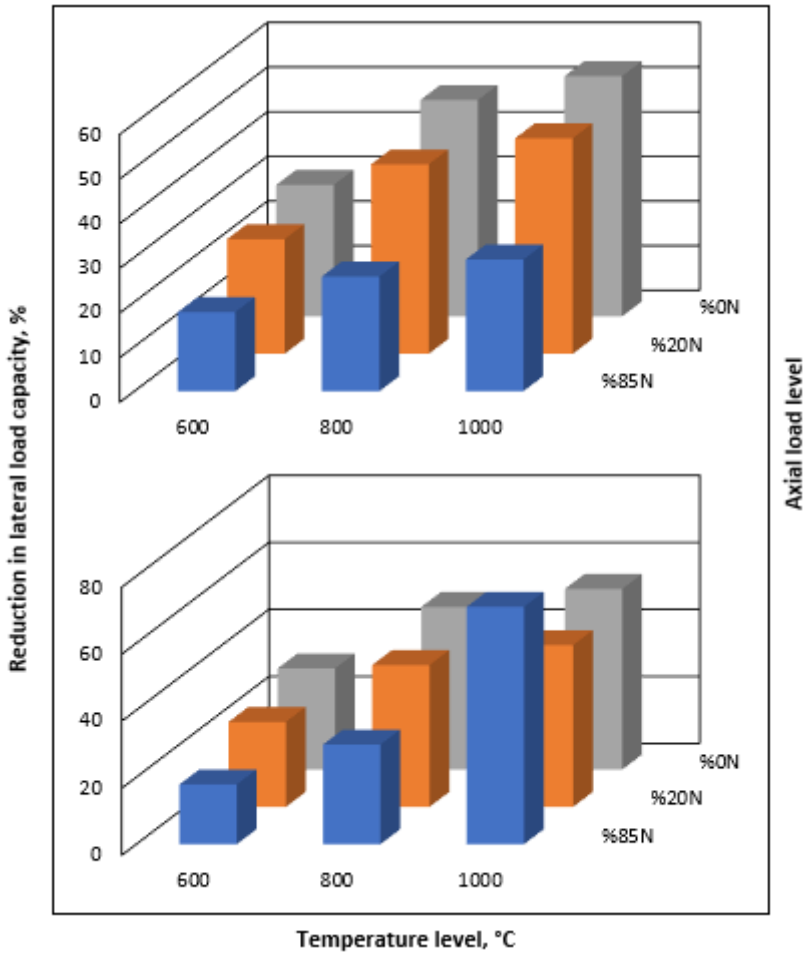

Figure 15. % reduction in lateral load carrying capacity of RC column

According to the data obtained as a result of thermo-mechanical analysis, the lateral load carrying capacity of RC column elements varies depending on the cross-sectional properties of the column element, the degree of temperature exposure and the axial load level.

Accordingly, in all column elements where the axial load level varies, the increase in temperature increases the decrease in the lateral load carrying capacity (Figure 15). In many studies in the literature [20, 47, 48], it has been determined that the load carrying capacity of all reinforced concrete columns, beams, slabs and frame elements exposed to high temperature effect decreases due to temperature increase and supports the present study. In addition, an increase in the axial load level increased the lateral load carrying capacity of both high-temperature and non-heat-exposed reference columns (Figure 15). In Table 5, the effect levels of the factors that are effective in the change of the lateral load carrying capacity of the RC column are shown for the pushover case.

3.3 Stiffness - horizontal displacement curve of RC column

The change in the stiffness of RC column elements subjected to high temperature is shown in Figure 16 if they are subsequently subjected to cyclic lateral loading effects at different axial load levels.

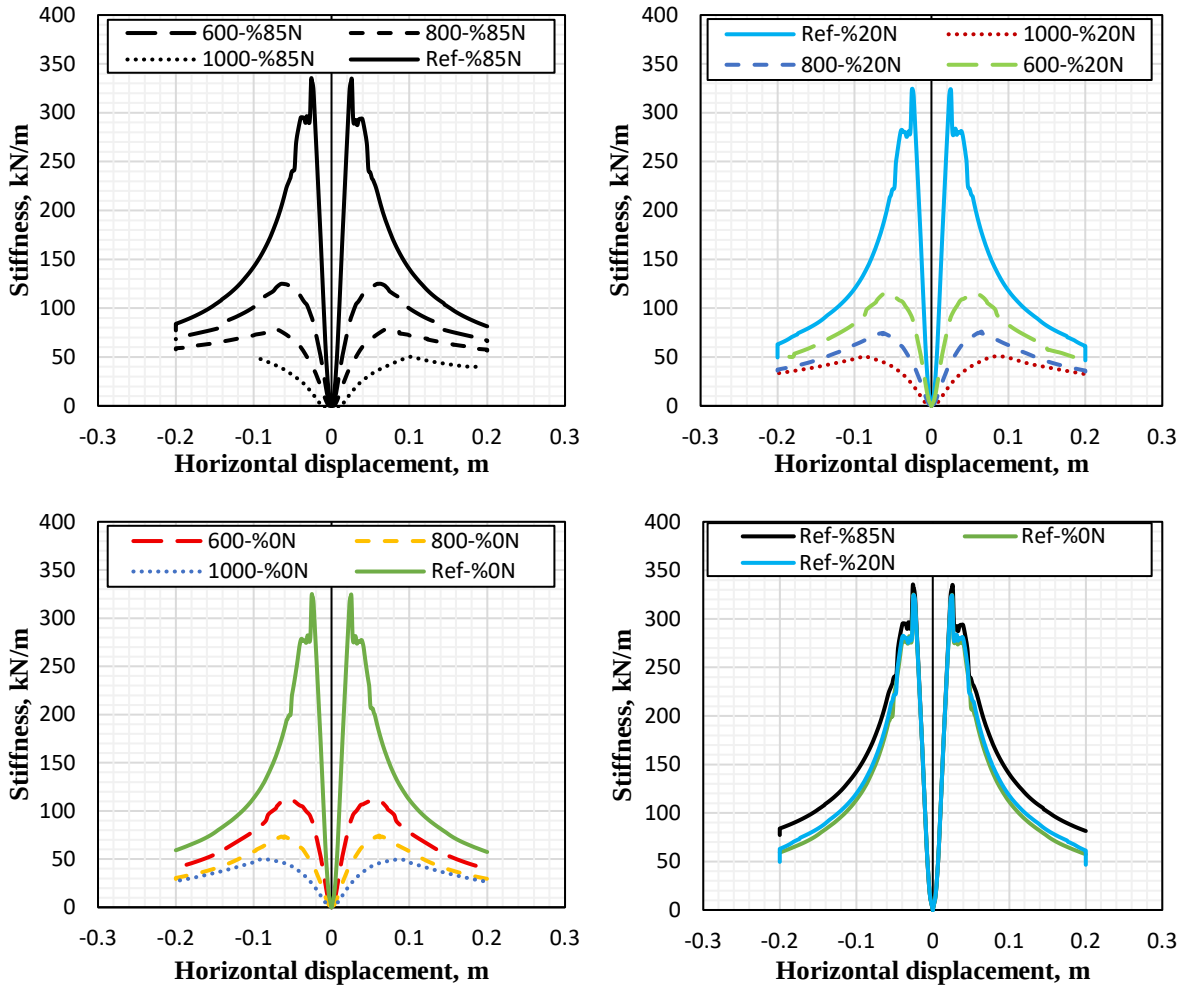

Figure 16. Temperature dependent variation of stiffness capacity of RC column

As a result of the thermal analysis, column stiffness decreased in all groups due to the increase in temperature. This reduction was obtained as 62.7%, 76.5% and 85% for pushing and pulling for 600, 800 and 1000 °C temperatures, respectively, for column elements where the axial load level was 85% of the column axial load capacity. It was determined that there was an average 64.5%, 76.8% and 84.3% reduction in thrust and shrinkage for 600, 800 and 1000 °C temperatures, respectively, in column elements where an axial load of 20% of the column axial load capacity was applied. The stiffness reduction in column elements without axial load was determined as 65.6%, 77.2% and 84.6% in push and pull for 600, 800 and 1000 °C temperatures, respectively. In similar studies in literature, stiffness losses in RC elements exposed to 600 and 800 °C high temperature for 180 minutes support the present study [47, 48]. The RC column element lost its remaining stiffness with the cyclic lateral loading analysis performed after the thermal analysis.

3.4 Effect of Axial Load Level on Cracking Mechanism and Stiffness Degradation of Reinforced Concrete Columns

The axial load level is one of the key parameters governing the cracking mechanism and the associated stiffness degradation of reinforced concrete columns subjected to lateral loading. In reference condition, an increase in axial load enhances the average compressive stress over the cross-section, which delays crack initiation in the tensile zone of concrete and limits crack propagation and opening. As a result, effective sectional stiffness is preserved

for a longer loading range, leading to higher initial stiffness values. Within the framework of the Concrete Damage Plasticity (CDP) model employed in this study, this behavior is reflected by a slower evolution of the tensile damage parameter (dt) and a relatively limited reduction in stiffness.

For columns exposed to elevated temperatures, significant reductions in the elastic modulus as well as in the compressive and tensile strengths of concrete accelerate crack initiation and intensify post-cracking stiffness degradation. The coupled thermo-mechanical analyses indicate that increasing temperature activates both tensile (dt) and compressive (dc) damage parameters at earlier stages, resulting in a rapid and generalized stiffness loss. While higher axial load levels partially restrain crack development and delay stiffness degradation at 600 and 800 °C, this beneficial effect becomes negligible at 1000 °C due to severe material degradation. At this temperature level, stiffness loss is largely independent of the axial load ratio and is primarily governed by fire-induced damage to the concrete material.

Moreover, although high axial load levels suppress crack opening at early loading stages, the accompanying increase in compressive damage (dc) associated with concrete crushing leads to inevitable stiffness degradation at larger deformation demands. These findings demonstrate that while axial load contributes positively to the preservation of initial stiffness at low and moderate temperature levels, the post-fire seismic behavior of reinforced concrete columns at advanced damage states is predominantly controlled by material deterioration rather than by axial load effects. Consequently, the interaction between axial load, cracking, and stiffness degradation should be explicitly considered in performance-based assessments of reinforced concrete columns subjected to fire and subsequent seismic loading.

IV. CONCLUSIONS

In this study, the post-fire behavior of reinforced concrete columns exposed to temperatures of 600, 800, and 1000 °C for 180 minutes following the ISO 834 standard fire curve, which was numerically investigated under cyclic lateral loading. The main findings of the study can be summarized as follows:

1. As the fire temperature increased, the lateral load-carrying capacity of reinforced concrete columns significantly decreased, reaching approximately 54% at a temperature of 1000 °C.
2. For columns exposed to 1000 °C, the variation in lateral load-carrying capacity was found to be independent of the axial load level, whereas at 600 and 800 °C, the capacity loss was dependent on the axial load. The smallest reduction in lateral load-carrying capacity was observed in the column exposed to 600 °C with a high axial load level.
3. For all temperature and axial load levels considered, the reduction in lateral load-carrying capacity exceeded the 15% threshold commonly associated with collapse conditions. Therefore, reinforced concrete columns exposed to temperatures of 600 °C and above for extended durations should not be reused without strengthening.
4. The stiffness capacity of reinforced concrete columns decreased by up to approximately 85% with increasing temperature, while the effect of axial load level on stiffness degradation was found to be limited.

5. These findings indicate that reinforced concrete columns subjected to fire experience a severe degradation in seismic performance. Accordingly, for engineering practice, it is essential to re-evaluate the lateral load and stiffness capacities of columns in post-fire structures through detailed structural analyses, and to make strengthening or decommissioning decisions based on performance-based assessment frameworks.

V. RECOMMENDATIONS FOR FUTURE STUDIES

1. Investigation of the behavior of RC columns exposed to 20, 200, 400, 600 and 800 °C high temperatures for 1, 2, 3 and 4 hours under different constant axial load and cyclic lateral load
2. Experimental and analytical investigation of the change in axial load carrying capacity of RC columns heated using different high temperature function curves
3. Experimental investigation of the structural behavior of RC columns simultaneously subjected to combined bending and ISO 834 standard fire
4. Determination of the time required for a RC column exposed to ISO 834 standard fire to reach the collapse state and investigation of fire performance

REFERENCES

1. Phan LT, Lawson JR, Davis FL (2001) Effects of elevated temperature exposure on heating characteristics, spalling, and residual properties of high performance concrete. Mater Struct 34:83-91.
2. Noumowe AN, Clastres P, Debicki G, Bolvin M (1994) High temperature effect on high performance concrete (70-600 C) strength and porosity. Spec Publ 145:157-172.
3. Shao S, Wasantha PL, Ranjith PG, Chen BK (2014) Effect of cooling rate on the mechanical behavior of heated Strathbogie granite with different grain sizes. Int J Rock Mech 70:381-387.
4. Yin W, Feng Z, Zhao Y (2021) Effect of grain size on the mechanical behaviour of granite under high temperature and triaxial stresses. Rock Mech Rock Eng 54:745-758.
5. Erdoğan TY (1985) Aggregates, the Turkish ready mixed concrete association. Istanbul, Turkey.
6. Malhotra HL (1956) The effect of temperature on the compressive strength of concrete. Mag Concr Res 8(23):85-94.
7. Aköz F, Yüzer N, Koral S (1995) The in fluence of high temperature on the physical and mechanical properties of ordinary Portland cement and silica fume mortar. Tech J Turk Chamb Civ Eng Tmmob Insaat Muhendisleri Odasi 6:287–292.
8. Akman MS (1987) Materials of construction. Istanbul Technical University Press, Istanbul.
9. Akman S (2000) Yapı hasarları ve onarım ilkeleri. TMMOB İnşaat Mühendisleri Odası İstanbul Şubesi.
10. Samadhiya A, Bhunia D, Chakraborty S (2024) Alkali-Activation Potential of Sandstone Wastes with Electric Arc Furnace Slag as Co-additive. Arab J Sci Eng 49(4):5817-5833.
11. Samadhiya A, Bhunia D, Chakraborty S, Lahoti M (2024) Influence of activator ratios and concentration on the physio-mechanical and microstructural characteristics of the geopolymers derived from sandstone processing waste. ESPR, 1-16.
12. Gautam PK, Singh SP, Agarwal A, Singh TN (2022) Thermomechanical characterization of two Jalore granites with different grain sizes for India's HLW disposal. Bull Eng Geol Environ 81(11):457.
13. Li Q, Wang M, Sun H, Yu G (2021) Effect of heating rate on the free expansion deformation of concrete during the heating process. J Build Eng 34:101896.
14. Arioz O (2007) Effects of elevated temperatures on properties of concrete. Fire Saf J 42(8):516-522.
15. Biolzi L, Cattaneo S, Rosati G (2008) Evaluating residual properties of thermally damaged concrete. Cem Concr Compos 30(10):907-916.
16. Felicetti R, Gambarova PG, Meda A (2009) Residual behavior of steel rebars and R/C sections after a fire. Constr. Build. Mater. 23(12):3546-3555.
17. Topçu İB, Karakurt C (2008) Properties of reinforced concrete steel rebars exposed to high temperatures. Adv Mater Sci Eng 2008(1):814137.
18. Bingöl AF, Gül R (2009) Residual bond strength between steel bars and concrete after elevated temperatures. Fire Saf J 44(6):854-859.

19. Chen YH, Chang YF, Yao GC, Sheu MS (2009) Experimental research on post-fire behaviour of reinforced concrete columns. Fire Saf J 44(5):741-748.
20. Ergün A, Kürklü G, Başpınar MS (2016) The effects of material properties on bond strength between reinforcing bar and concrete exposed to high temperature. Constr Build Mater 112:691-698.
21. Kodur VKR, Agrawal A (2016) An approach for evaluating residual capacity of reinforced concrete beams exposed to fire. Eng Struct 110:293-306.
22. Jiang CJ, Yu JT, Li LZ, Wang X, Wang L, Liao JH (2018) Experimental study on the residual shear capacity of fire-damaged reinforced concrete frame beams and cantilevers. Fire Saf J 100:140-156.
23. Jau WC, Huang KL (2008) A study of reinforced concrete corner columns after fire. Cem Concr Compos 30(7):622-638.
24. Dong Y, Fan W, Wang Q, Yang B (1996) Study on residual load-bearing capacity and reliability index of reinforced concrete slab post-fire. Fire Saf Sci 5:7-11.
25. Pul S, Atasoy A, Senturk M, Hajirasouliha I (2021) Structural performance of reinforced concrete columns subjected to high-temperature and axial loading under different heating-cooling scenarios. J Build Eng 42:102477.
26. ISO 834 (2014). Fire Resistance Tests Elements of Building Construction, Geneva, International Organization for Standardization (ISO). ISO 834
27. Abaqus/CAE V6.12 (2018) Programme, Dassault Systemes Simulia Corp. Providence, RI, USA.
28. Türkiye Bina Deprem Yönetmeliği, Afet ve Acil Durum Yönetimi Başkanlığı, Ankara, 2018.
29. TS EN 1992 – 1 – 2 (2004). Eurocode 2: Design of concrete structures – Part 1 – 2: General rules – Structural fire design.
30. TS EN 1993 – 1 – 2 (2005). Eurocode 3: Design of steel structures – Part 1 – 2: General rules – Structural fire design.
31. Vitorino H, Rodrigues H, Couto C (2020) Evaluation of post-earthquake fire capacity of a reinforced concrete one bay plane frame under ISO fire exposure. Struct. 23:602-611.
32. Kamath P, Sharma UK, Kumar V, Bhargava P, Usmani A, Singh B, et al (2015) Full-scale fire test on an earthquake-damaged reinforced concrete frame. Fire Saf J 73:1-19.
33. Shah AH, Sharma UK, Bhargava P (2017) Outcomes of a major research on full scale testing of RC frames in post earthquake fire. Constr Build Mater 155:1224-1241.
34. Parthasarathi N, Satyanarayanan KS (2020) Progressive collapse behavior of reinforced concrete frame exposed to high temperature. J Struct Fire Eng 12(1):110-124.
35. Çolakoğlu HE, Hüsem M (2025) Investigation of the cyclic load behavior of reinforced concrete frames exposed to high temperatures using the finite element method. Sigma 43(3):857-877.
36. Ren W, Sneed LH, Yang Y, He R (2015) Numerical simulation of prestressed precast concrete bridge deck panels using damage plasticity model. IJCSM, 9:45-54.
37. Zhao G, Zhang M, Li Y, Li D (2016) The hysteresis performance and restoring force model for corroded reinforced concrete frame columns. J Eng 2016(1):7615385.
38. Michał S, Andrzej W (2015) Calibration of the CDP model parameters in Abaqus. World Congress on Advances in Structural Engineering and Mechanics (ASEM 15), Incheon Korea.
39. Filippo MD (2016) Non-linear static and dynamic finite element analyses of reinforced concrete structures, Alborg University.
40. Dere Y, Koroglu MA (2017) Nonlinear FE modeling of reinforced concrete. IJSCER, 6(1):71-74.
41. Labibzadeh M, Zakeri M, Adel Shoaib A (2017) A new method for CDP input parameter identification of the ABAQUS software guaranteeing uniqueness and precision. Int J Struct 8(2):264-284.
42. Teklemariam DM, Hamunzala B (2016) Design of Thick Concrete Beams: Using Non-Linear FEM.
43. Sümer Y, Aktaş M (2015) Defining parameters for concrete damage plasticity model. Chall J Struct Mech 1(3):149-155.
44. Applied Technology Council, Mid-America Earthquake Center, Multidisciplinary Center for Earthquake Engineering Research (US), Pacific Earthquake Engineering Research Center, & National Earthquake Hazards Reduction Program (US). (2007). Interim testing protocols for determining the seismic performance characteristics of structural and nonstructural components. Federal Emergency Management Agency.
45. JGJ 138-2001 (2001) Technical specification for steel reinforced concrete composite structures.
46. Belkacem MA, Bechtoula H, Bourahla N, Belkacem AA (2019) Effect of axial load and transverse reinforcements on the seismic performance of reinforced concrete columns. Front Struct Civ Eng 13:831-851.
47. Jau WC, Huang KL (2008) A study of reinforced concrete corner columns after fire. Cem Concr Compo. 30(7):622-638.
48. Çolakoğlu HE, Hüsem M, Demir S, Akbulut YE, Yılmaz Y (2024) The behavior of reinforced concrete frames exposed to high temperature under cyclic load effect. Struct 63:106446.